Progress In Electromagnetics Research, PIER 55, 33–46, 2005

WIDEBAND AND EFFICIENT MICROSTRIP INTERCONNECTS USING MULTI-SEGMENTED GROUND AND OPEN TRACES

M. Khalaj-Amirhosseini and A. Cheldavi

College of Electrical Engineering
Iran University of Science and Technology
Tehran, Iran

Abstract—In this paper, two new interconnect structures called Multi-Segmented S-G-S (Signal-Ground-Signal) and S-O-S (Signal-Open-Signal) interconnects are proposed and compared with the conventional S-S-S interconnects. In these interconnect structures a multi-segmented grounded or opened line is inserted between two adjacent signal lines. The grounded (opened) lines have been grounded (opened) not only in their terminals, but also in some places along their length. The performances of these interconnects are studied via some examples.

1. INTRODUCTION

With the development of microwave VLSI circuits, there is a significant interest in the design and manufacturing suitable interconnect structures to reduce the crosstalk in the adjacent lines while maximize the delivered power in the main line. An interconnect structure is a multi-conductor coupled transmission line designed to transfer several signals from the main die to the users d meters far from the die. Many efforts have been done to design interconnects that have low crosstalk power while the delivered power in the main line has been maximized [1–12]. Some of the important types of interconnects introduced are denoted as S-G-S, G-S-G and S-G-G-S [8–11] where S represents the signal traces and G represents additional ground traces. The ground traces are additional lines that have been grounded in their two ends. Usually the ground traces contain $K = 1$ segment (only two grounded points in their terminals).

In this paper, we propose S-O-S type structure, in which O represents open traces, which are opened or floated additional lines. Also, the S-G-S and the proposed S-O-S structures are discussed in a case that the ground or open traces have been made from several segments, i.e., $K \geq 1$ segments (more than two grounded or opened points along their length). Finally, using some examples some results are given about wideband and efficient design of interconnects subject to constant total width, W_T.

2. INTERCONNECTS PERFORMANCE ANALYSIS

In the interconnects, the power transferred to the load of the excited signal trace and the crosstalk power transferred to the loads of the other idle signal traces are very important because they represent the overall functional performance. Fig. 1 shows the cross section and longitudinal view of a conventional microstrip interconnects, i.e., S-S-S type, with N signal traces and total width of W_T. Figs. 2 and 3 show the cross

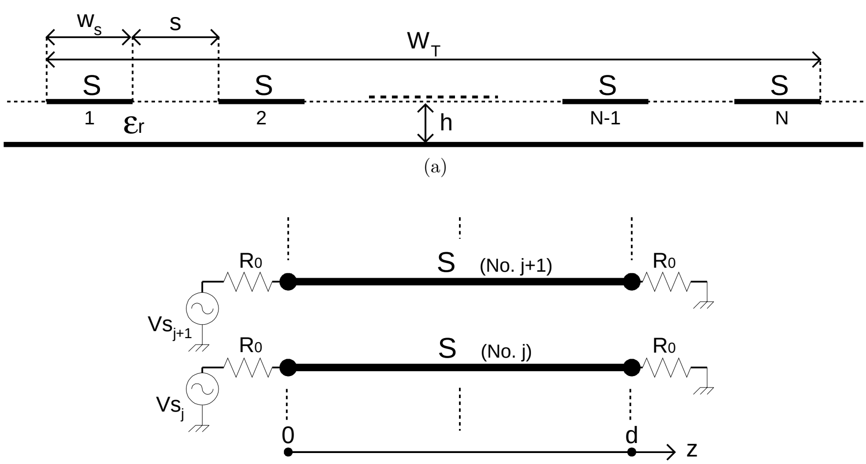

(b)

Figure 1. Conventional S-S-S type microstrip interconnects a) The cross section b) Longitudinal view.

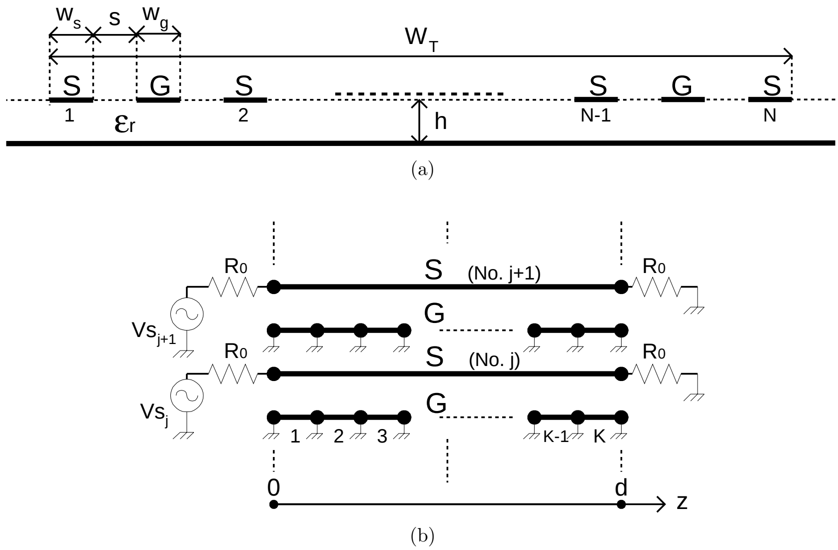

Figure 2. The S-G-S type microstrip interconnects a) The cross section b) Longitudinal view.

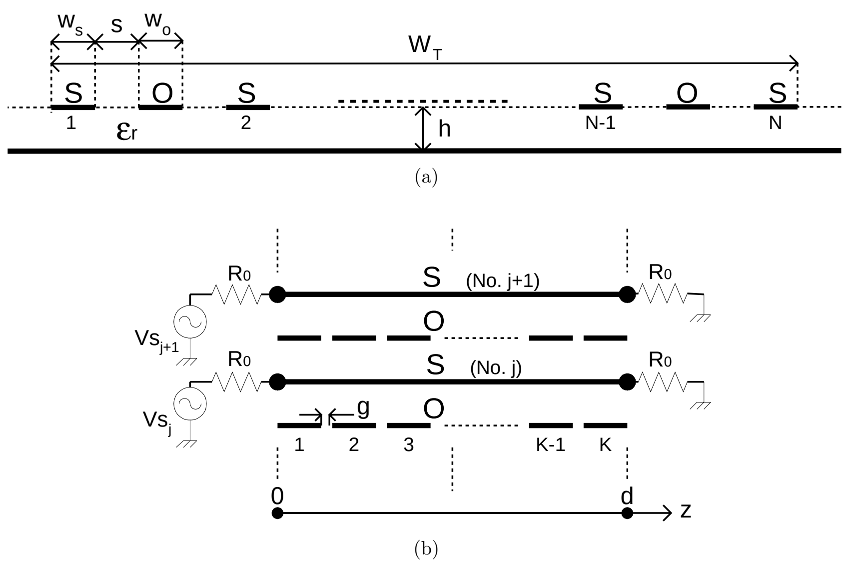

Figure 3. The S-O-S type microstrip interconnects a) The cross section b) Longitudinal view.

section and longitudinal view of S-G-S and S-O-S types interconnects, respectively. These interconnects contain N signal traces and $N-1$ open or ground traces each with K segments. The thickness and the relative electric permittivity of the substrate are h and ε_r, respectively. The widths of all signal, ground and open traces are w_s, w_g and w_o, respectively and total width is W_T. Also, the length of traces is d and the distances between them are s. It is assumed all signal traces have been loaded by resistor R_0, at their two-ends. The gap g between two adjacent open segments should be as small as possible ($g \ll d/K$) to reduce the crosstalk, while having very large capacitive impedance for considering it as an open segment.

To study the performances of the above interconnects, it is needed to analyze $2N-1$ coupled transmission lines as shown in Fig. 3. First, we define voltage, current and source voltage vectors, respectively as

$$\boldsymbol{V}(z,\omega) = [V_1(z,\omega) \quad V_2(z,\omega) \quad \dots \quad V_{2N-1}(z,\omega)]^T \tag{1a}$$

$$\boldsymbol{I}(z,\omega) = [I_1(z,\omega) \quad I_2(z,\omega) \quad \dots \quad I_{2N-1}(z,\omega)]^T \tag{1b}$$

$$\boldsymbol{V}_S = [V_{S_1} \quad 0 \quad V_{S_2} \quad 0 \quad \dots \quad 0 \quad V_{S_N}]^T \tag{2}$$

The terminal conditions are as follows

$$\begin{aligned} \boldsymbol{V}(0,\omega) &= \boldsymbol{V}_S - \boldsymbol{Z}_S \boldsymbol{I}(0,\omega) \\ \boldsymbol{V}(d,\omega) &= \boldsymbol{Z}_L \boldsymbol{I}(d,\omega) \end{aligned} \tag{3}$$

in which $\boldsymbol{Z}_L$ and $\boldsymbol{Z}_S$ are two $(2N-1)\times(2N-1)$ diagonal matrices as follows

$$\boldsymbol{Z}_L = \boldsymbol{Z}_S = \begin{cases} \mathrm{diag}(R_0 \quad 0 \quad R_0 \quad 0 \quad \dots \quad 0 \quad R_0) & ;\ \text{S-G-S type} \\ \mathrm{diag}(R_0 \quad \infty \quad R_0 \quad \infty \quad \dots \quad \infty \quad R_0) & ;\ \text{S-O-S type} \end{cases} \tag{4}$$

On the other hand, one can write

$$\begin{bmatrix} \boldsymbol{V}(d,\omega) \\ \boldsymbol{I}(d,\omega) \end{bmatrix} = \boldsymbol{\Phi} \begin{bmatrix} \boldsymbol{V}(0,\omega) \\ \boldsymbol{I}(0,\omega) \end{bmatrix} \tag{5}$$

in which

$$\boldsymbol{\Phi} = \begin{bmatrix} \boldsymbol{\varphi}_{11} & \boldsymbol{\varphi}_{12} \\ \boldsymbol{\varphi}_{21} & \boldsymbol{\varphi}_{22} \end{bmatrix} \tag{6}$$

is the chain parameter matrix of the interconnect. According to Fig. 3, this matrix can be represented as

$$\boldsymbol{\Phi} = \boldsymbol{\Phi}_L \left(\prod_{k=1}^{K-1} \boldsymbol{\Phi}_{go} \boldsymbol{\Phi}_L \right) \tag{7}$$

In (7), $\boldsymbol{\Phi}_L$ is the $2(2N-1)\times 2(2N-1)$ chain parameter matrix of each segment of the interconnect, as follows [13]

$$\boldsymbol{\Phi}_L = \mathbf{exp}\left(-j\omega\frac{d}{K}\begin{bmatrix} \mathbf{0} & \boldsymbol{L} \\ \boldsymbol{C} & \mathbf{0} \end{bmatrix}\right) \tag{8}$$

and $\boldsymbol{\Phi}_{go}$ is the chain parameter matrix of grounded or opened points along the length of interconnects. In (8), $\boldsymbol{L}$ and $\boldsymbol{C}$ are the per-unit-length inductance and capacitance matrices, respectively. The chain parameter matrix in (8) can be calculated using eigen-value decomposition or the modal decomposition methods [13]. Also, the matrix $\boldsymbol{\Phi}_{go}$ can be represented as

$$\boldsymbol{\Phi}_{go} = \begin{bmatrix} \boldsymbol{a} & \boldsymbol{b} \\ \boldsymbol{c} & \boldsymbol{d} \end{bmatrix} \tag{9}$$

in which its sub-matrices are $(2N-1)\times(2N-1)$ diagonal matrices as follows

$$\boldsymbol{a} = \boldsymbol{d} = \mathrm{diag}(\ldots \quad 1 + z_s/z_p \quad \ldots) \tag{10a}$$

$$\boldsymbol{b} = \mathrm{diag}(\ldots \quad -z_s \quad \ldots) \tag{10b}$$

$$\boldsymbol{c} = \mathrm{diag}(\ldots \quad -(2 + z_s/z_p)/z_p \quad \ldots) \tag{10c}$$

In (10), z_s and z_p are respectively the series and parallel impedances of Π type circuit model of the discontinuities at the ends of each segment, given by

$$z_s = \begin{cases} 0 & ; \quad \text{for the signal traces} \\ 0 & ; \quad \text{for the ground traces} \\ 1/(j\omega C_g) & ; \quad \text{for the open traces} \end{cases} \tag{11}$$

and

$$z_p = \begin{cases} \infty & ; \quad \text{for the signal traces} \\ 2R_V & ; \quad \text{for the ground traces} \\ 1/(j\omega C_p) & ; \quad \text{for the open traces} \end{cases} \tag{12}$$

In (11) and (12), R_V is the small resistance of the grounded vias and C_g and C_p are the small capacitances in the circuit model of the gaps, both have been shown in Fig. 4.

Incorporating (3) and (5), leads to far-end terminal voltages of the lines as follows

$$\boldsymbol{V}(d,\omega) = \boldsymbol{F}\boldsymbol{V}_S \tag{13}$$

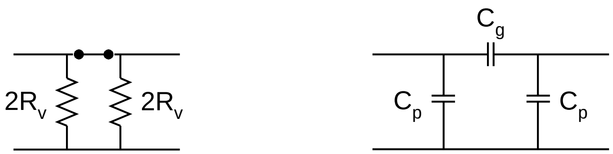

Figure 4. The circuit model of the vias (left hand) and the gaps (right hand), respectively in S-G-S and S-O-S type interconnects.

in which $\boldsymbol{F}$ is an $N \times N$ matrix as follows

$$\begin{aligned}\boldsymbol{F} &= \boldsymbol{Z}_L\varphi_{21} - \boldsymbol{Z}_L(\varphi_{22} - \varphi_{21}\boldsymbol{Z}_S) \\ &\quad \times(\varphi_{12}-\varphi_{11}\boldsymbol{Z}_S-\boldsymbol{Z}_L\varphi_{22}+\boldsymbol{Z}_L\varphi_{21}\boldsymbol{Z}_S)^{-1}(\varphi_{11}-\boldsymbol{Z}_L\varphi_{21}) \quad (14)\end{aligned}$$

After finding terminal voltages of interconnects, we can study their performances. In order to study the overall performance of interconnects; we define the following performance factors as a function of the frequency f.

$$\eta_{LA}(f) = 10\log\left(\frac{P_L(f)}{P_A}\right) \quad [\text{dB}] \tag{15a}$$

$$\eta_{CA}(f) = 10\log\left(\frac{P_C(f)}{P_A}\right) \quad [\text{dB}] \tag{15b}$$

in which P_A, P_L and P_C are the total available power, total power delivered to the far-end loads and total far-end crosstalk power delivered to the loads, when all N sources are applied separately. These powers can be obtained using the matrix $\boldsymbol{F}$ defined in (14) as follows

$$P_A = \frac{N}{8R_0} \tag{16a}$$

$$P_L(f) = \frac{1}{2R_0}\sum_{\substack{i=1\\ i=odd}}^{2N-1}\left(|\boldsymbol{F}(i,i;f)|^2\right) \tag{16b}$$

$$P_C(f) = \frac{1}{2R_0}\sum_{\substack{i=1\\ i=odd}}^{2N-1}\ \sum_{\substack{j=1\\ j=odd\\ j\neq i}}^{2N-1}\left(|\boldsymbol{F}(i,j;f)|^2\right) \tag{16c}$$

3. EXAMPLES AND RESULTS

As an example, an S-G-S type and an S-O-S type microstrip interconnect are analyzed and compared with an S-S-S type microstrip interconnect while all have the same total width W_T. Consider an S-G-S or S-O-S interconnect with $N = 5$ signal traces, $\varepsilon_r = 10$, $w_s/h = w_g/h = w_o/h = s/h = 0.529$ ($W_T = 9h$) and the loads $R_0 = 50\,\Omega$. Assume the length of this interconnect to be $d = 10\,\text{cm}$ and the ground and open traces have $K = 1$, 2, 3 and 4 segments. Figs. 5 and 6 show the performance factors η_{LA} and η_{CA}, respectively for the S-G-S type interconnect. Also, Figs. 7 and 8 show the performance factors η_{LA} and η_{CA}, respectively for the S-O-S type interconnect. In these four figures, the performance factors of these two types interconnects are compared with those of a S-S-S type interconnect with $w_s/h = s/h = 1$ ($W_T = 9h$).

The width of the strips and the distances between them can be chosen arbitrary so to have an optimum design for S-S-S, S-G-S and S-O-S types interconnects. To get to the optimum design for the above example, Figs. 9 and 10 show the contours of minimum values of η_{LA} in frequencies from zero to 500 MHz (near the first null in η_{LA}) for S-G-S and S-O-S types interconnects, respectively. Also, Figs. 11 and 12 show the contours of maximum values of η_{CA} over frequencies from zero to 500 MHz for S-G-S and S-O-S types interconnects, respectively. In Figs. 9–12, the relative distance between the strips, s/h, are chosen so that the total width of the interconnects to be fixed as $W_T = 9h$.

From Figs. 5–12 one may conclude the following results:

1. One can find some optimum values for the width of signal, ground and open traces to get to arbitrary large η_{LA} and arbitrary small η_{CA}. So, the performance factors of the S-G-S and S-O-S types interconnects can be much better than those of the conventional S-S-S type interconnects. Thus the width of signal and ground or open traces of the S-G-S and S-O-S types interconnects can be selected to get to more better values for η_{LA} and η_{CA} than S-S-S type interconnects.
2. The S-G-S type interconnects can be designed to have more better performance factors than the S-O-S type interconnects. Of course, the fabrication process of the S-O-S type interconnects is much more simpler than the S-G-S type interconnects. So, it is better to use S-G-S type rather than S-O-S type interconnect in the expense of more fabrication cost for grounded vias.
3. Both performance factors of S-G-S and S-O-S types interconnects become undesirable in some frequencies. These undesirable frequencies are the same as the resonance frequencies of the

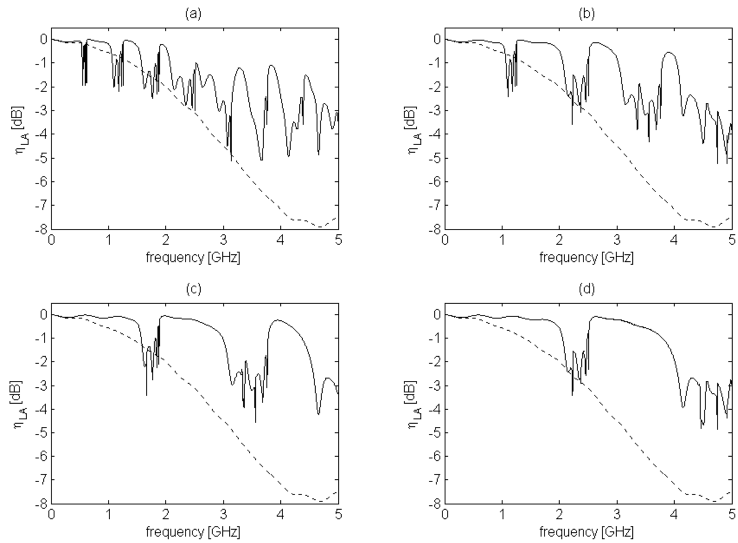

Figure 5. The delivered power performance factor η_{LA} for the S-G-S (the full lines) and S-S-S (the dotted lines) structures a) $K = 1$ b) $K = 2$ c) $K = 3$ d) $K = 4$ segments.

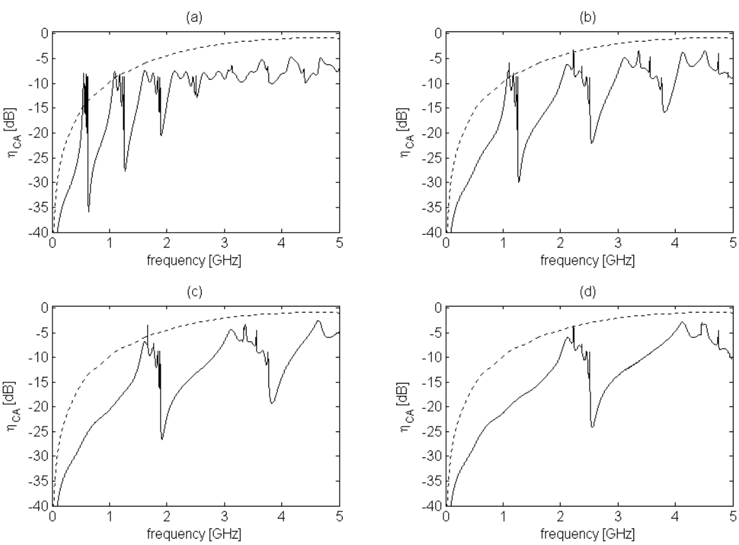

Figure 6. The crosstalk power performance factor η_{CA} for the S-G-S (the full lines) and S-S-S (the dotted lines) structures a) $K = 1$ b) $K = 2$ c) $K = 3$ d) $K = 4$ segments.

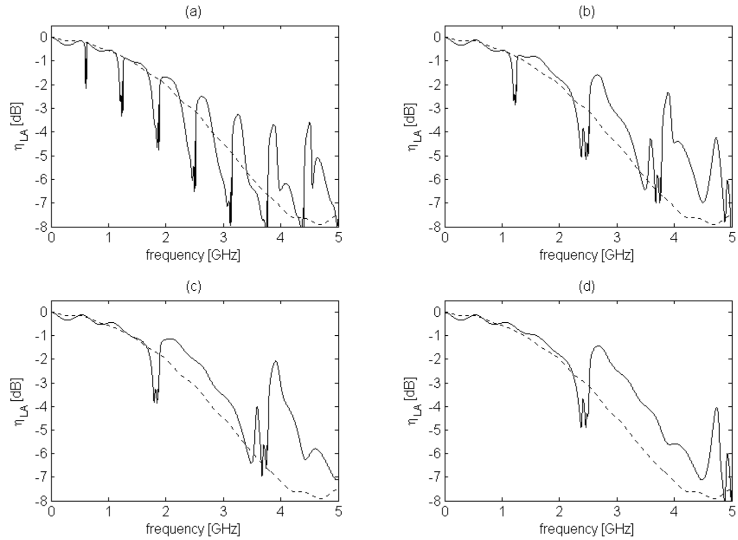

Figure 7. The delivered power performance factor η_{LA} for the S-O-S (the full lines) and S-S-S (the dotted lines) structures a) $K = 1$ b) $K = 2$ c) $K = 3$ d) $K = 4$ segments.

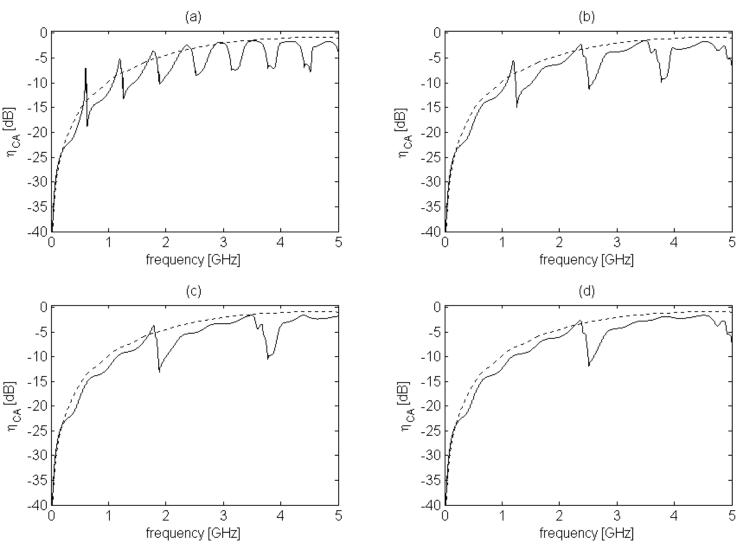

Figure 8. The crosstalk power performance factor η_{CA} for the S-O-S (the full lines) and S-S-S (the dotted lines) structures a) $K = 1$ b) $K = 2$ c) $K = 3$ d) $K = 4$ segments.

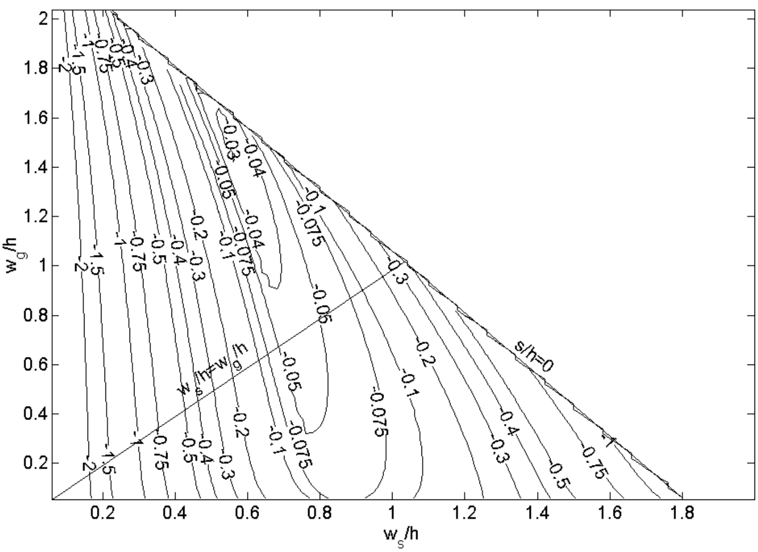

Figure 9. Contours of minimum values of η_{LA} over frequencies from zero to 500 MHz for S-G-S interconnect.

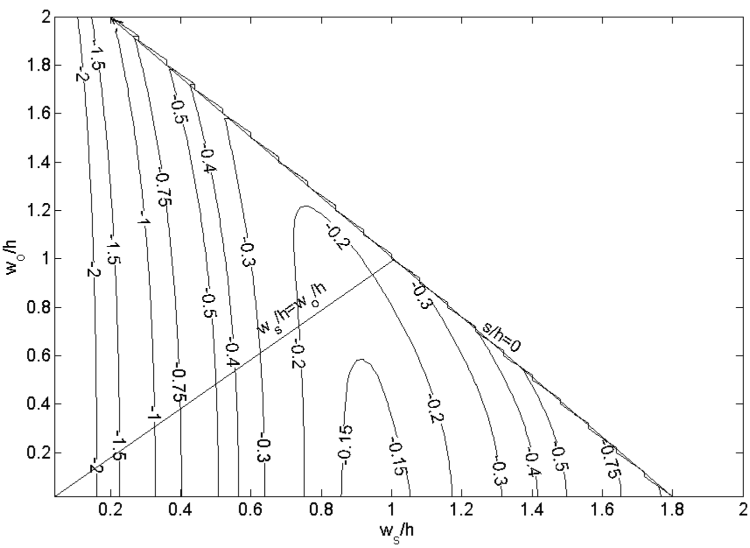

Figure 10. Contours of minimum values of η_{LA} over frequencies from zero to 500 MHz for S-O-S interconnect.

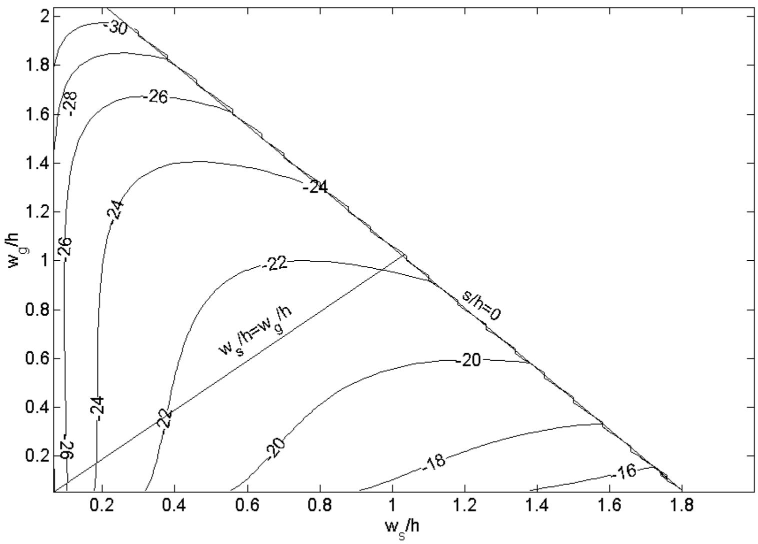

Figure 11. Contours of maximum values of η_{CA} over frequencies from zero to 500 MHz for S-G-S interconnect.

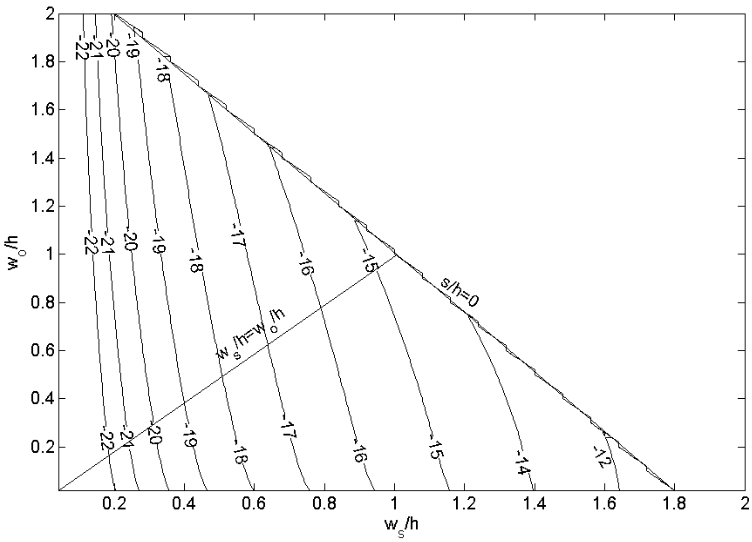

Figure 12. Contours of maximum values of η_{CA} over frequencies from zero to 500 MHz for S-O-S interconnect.

grounded or opened lines. This resonance phenomenon occurs in frequencies that the length of the grounded or opened lines becomes multiple of a half of the effective wavelength. In fact,

$$f_{undesirable} = nK \frac{c}{2d\sqrt{\varepsilon_{re}}} \quad ; \quad n = 1, 2, 3, \ldots \tag{17}$$

in which c is the velocity of the light and ε_{re} is the effective permittivity of the loaded microstrip lines (in this example 6.5). The frequency bandwidth of S-G-S and S-O-S types of interconnects is from zero to the first undesirable frequency. From (17), it is resulted that if the number of segments K along the length of S-G-S and S-O-S types of interconnects increases (using grounded vias in ground traces or simple gaps in open traces), the position of the first undesirable frequency will be increased. So, getting the length of each segment smaller and smaller, the frequency bandwidth of interconnects becomes wider and wider.

It is worthy to mention that, although the width of signal traces of S-G-S and S-O-S types of interconnects is narrower than that of S-S-S type interconnects, the characteristic impedance of S-G-S and S-O-S types can be very near the characteristic impedance of S-S-S types. This is because the distance between two adjacent traces in S-G-S and S-O-S types is smaller than those of S-S-S types.

4. CONCLUSION

Two new Multi-Segmented S-G-S and S-O-S interconnect structures are proposed. Two performance factors have been defined and obtained for a S-G-S and a S-O-S interconnect with $K = 1, 2, 3$ and 4 segments in the ground or open traces. The results show that these structures have very better performance factors than those of the simple conventional S-S-S structures for the same total width. The frequency bandwidth of S-G-S and S-O-S interconnects will be magnified if the number of the line segments in ground or open traces is increased.

REFERENCES

1. Gazizov, "Far-end crosstalk reduction in doubled-layered dielectric interconnects," *IEEE Trans. Electromag. Comp.*, 566–572, 2001.
2. Gilb, J. P. K. and C. A. Balanis, "Pulse distortion on multiplayer coupled microstrip lines," *IEEE Trans. Microwave Theory and Tech.*, 1620–1628, Oct. 1989.

3. Gilb, J. P. K. and C. A. Balanis, "Asymmetric, multi-conductor low-coupling structures for high-speed, high-density digital interconnects," *IEEE Trans. Microwave Theory and Tech.*, 2100–2106, Dec. 1991.
4. Weirather, R. R., "A small MIC coupler with with good directivity," *IEEE Trans. Microwave Theory and Tech.*, 70–71, Jan. 1974.
5. Novak, I., B. Eged, and L. Hatvani, "Measurement and computer simulation of discrete discontinuities along coupled PCB traces," *IEEE Conf. Instrumentation and Measurement and Technology Conference*, 385–385D, Irvine, CA, May 1993.
6. Gipprich, J. and D. Stevens, "A new via fence structure for crosstalk reduction in high density stripline packages," *IEEE MTT-S Int. Mic. Symp. Dig.*, 1719–1722, 2001.
7. Qian, Y. and G. Yamashita, "Characterization of picosecond pulse crosstalk between coupled microstrip lines with arbitrary conductor width," *IEEE Trans. Microwave Theory and Tech.*, 1011–1016, June/July 1993.
8. Khalaj Amirhosseini, M. and A. Cheldavi, "Effiecient interconnect design using grounded-lines," *J. of Electromagn. Waves and Appl.*, 1289–1300, Sept. 2003.
9. You, H. and M. Soma, "Crosstalk analysis of interconnection lines and packages in high speed integrated circuits," *IEEE Trans. Circuits and Systems*, 1019–1026, Aug. 1990.
10. Novak, I., B. Eged, and L. Hatvani, "Measurement and simulation of crosstalk reduction by discrete discontinuities along coupled PCB traces," *IEEE Trans. Instrum. Measur.*, No. 2, 170–175, 1994.
11. Khalaj Amirhosseini, M. and A. Cheldavi, "Optimum and wideband design of G-S-G interconnects," *Proc. IASTED int. Conf. on Communication Systems and Networks*, 310–312, Marbella, Spain, Sept. 1–3, 2004.
12. Khalaj Amirhosseini, M. and A. Cheldavi, "Optimum design of microstrip RF interconnects," *J. of Electromagn. Waves and Appl.*, 1707–1715, Dec. 2004.
13. Paul, C. R., *Analysis of Multiconductor Transmission Lines*, John Wiley and Sons Inc., 1994.

Mohammad Khalaj-Amirhosseini was born in Tehran, Iran in 1969. He received his B.Sc. M.Sc. and Ph.D. degrees from Iran University of Science and Technology (IUST) in 1992, 1994, and 1998, respectively, all in electrical engineering. He is currently an Assistant Professor at Electrical Engineering Department of IUST. His scientific fields of interest are electromagnetic direct and inverse problems including wave propagation, high frequency circuits and systems, microwaves and antennas.

Ahmad Cheldavi was born in Ahwaz, a beautiful and hot city in south of Islamic Republic of Iran, in 1966. He received his B.Sc. degree (with honors) from Iran University of Science and Technology in 1992, the M.Sc. and Ph.D. degrees (with honors) from University of Tehran in 1994 and 2000, respectively, all in Electrical Engineering. He is currently an Associate Professor at Electrical Engineering Department of Iran University of Science and Technology. He is the author of more than 100 journal and conference papers in the fields of EMC, EMI, microwave transmission lines, application of genetic algorithms in electromagnetics, and coupled lines characterization.